EASR

Engineering and Applied Science Research

https://www.tci-thaijo.org/index.php/easr/index

Published by the Faculty of Engineering, Khon Kaen University, Thailand

Identification and quantification of quality of intact durian fruits using NIR spectroscopy

Lakkana Pitak[1)], Sirirak Ditcharoen[2)], Kanvisit Maraphum[1)], Buathip Khamwan[2)], Nithithada Warorost[2)], Yuwatida Sripontan[3)], Chun-I Chiu[4)], Panmanas Sirisomboon[5)] and Jetsada Posom*[2)]

[1)]Department of Agricultural Machinery, Faculty of Agriculture and Technology, Rajamangala University of Technology Isan Surin Campus, Surin, Thailand
[2)]Department of Agricultural Engineering, Faculty of Engineering, Khon Kaen University, Khon Kaen, Thailand
[3)]Department of Entomology and Plant Pathology, Faculty of Agriculture, Khon Kaen University, Khon Kaen, Thailand
[4)]Department of Entomology and Plant Pathology, Faculty of Agriculture, Chiang Mai University, Chiang Mai, Thailand
[5)]Department of Agricultural Engineering, School of Engineering, King Mongkut's Institute of Technology Ladkrabang, Bangkok, Thailand

Received 15 June 2025
Revised 15 October 2025
Accepted 17 October 2025

Abstract

Quality classification of durian fruits is based on the dry matter (DM) content of the pulp. According to Thai agricultural standards, durian fruit (Monthong variety) must contain at least 32% DM. This study aimed to develop a classification model for assessing durian quality based on DM content, categorizing fruits as either "rejected" (DM < 32%) or "accepted" (DM ≥ 32%). Near-infrared (NIR) spectra were collected as the durian fruits moved along a conveyor belt. The models were developed using two spectral ranges: short-wavelength near-infrared (SWNIR; 4501000 nm) and long-wavelength near-infrared (LWNIR; 8601750 nm). Owing to the imbalance in the dataset between the two classes, the data were adjusted using the synthetic minority oversampling technique to create a balanced dataset. Prediction models were built using different spectral preprocessing methods and algorithms. For the LWNIR range, the models constructed using LDA, SVM, KNN, and SDA achieved accuracies of 95%, 90%, 93%, and 93%, respectively, for the test set. The SWNIR models, developed using the same algorithms, achieved accuracies of 90%, 88%, 90%, and 90%, respectively, for the test set. PLS-regression was used to predict the DM content from both LWNIR and SWNIR data. With the 2nd derivative preprocessing method, the models achieved R^2 values of 0.89 and 0.79, SEP values of 5% and 6.89%, and RPD values of 2.29 and 1.66, respectively. The wavelength range significantly influenced the model performance, whereas spectral pretreatment had a minor effect on the model's predictive ability. Overall, NIR spectroscopy demonstrated the potential for nondestructive quality grading of whole durian fruits. This work is the first to establish real-time, in-line models for durian grading based on DM content, advancing beyond the previous destructive method. The findings demonstrate the feasibility of automated, nondestructive, and objective quality assessment, supporting industrial automation, precision agriculture, and export quality assurance.

Keywords: Durian, Nondestructive, Dry matter, Classification, Long-wave NIR, Short-wave NIR

1. Introduction

Durian (*Durio zibethinus*), often referred to as the "king of fruits", is a significant economic fruit in Thailand, enjoying widespread popularity and showing continuous growth [1]. According to the Department of Agriculture, Ministry of Agriculture and Cooperatives, the eastern region of Thailand was expected to produce no less than 700,000 tons of durians for export in the 2024 fruit season [1]. This output was achieved through coordinated efforts between the public and private sectors to control the production process and maintain the quality of Thai durians [1]. In 2024, Thailand's export of fresh durian products was projected to reach 800,000 tons [2]. Typically, durians are classified into two stages: mature and ripe. A ripe durian is considered ready to eat. Traditional techniques for determining ripeness are based on external appearance, such as the skin becoming darker and transitioning from green to light yellow or yellow when fully ripe. Additionally, a fully ripe durian may show cracks on the sides or spaces between the spikes, and the skin should feel slightly soft when gently pressed. The smell becomes more intense as the durian nears full ripeness [3].

For exports, only fully mature durians are shipped to ensure that they are perfectly ripe when they reach customers. According to the Ministry of Agriculture and Cooperatives Standard TAS 3-2013, "Monthong" durians are considered fully mature when their dry matter (DM) content is ≥32% [4, 5]. Therefore, the challenge in sorting lies in distinguishing fully mature durians from immature durians, which is typically more difficult than sorting ripe durians. Immature durians have a DM < 32%. The ripening period after harvest under natural conditions is approximately 6–9 days [5]. Classifying durians as having DM ≥ 32% or DM < 32% remains a challenge, and many researchers have explored this issue. The dry oven method has traditionally been used to determine the DM of fresh durian. However, this method is time-consuming and requires approximately 48 hours per sample. Durian fruits collected from

*Corresponding author.
Email address: jetspo@kku.ac.th
https://doi.org/10.64960/easr.2026.262620

farmers are randomly inspected, with one to two fruits typically tested to confirm maturity. This method is not only labor-intensive and destructive to the samples, but also affects the quality and quantity of the produce, and it cannot guarantee 100% accuracy.

The implementation of rapid quality screening methods may help maintain the quality of durians, reduce product losses, and enhance competitive pricing. Currently, near-infrared (NIR) spectroscopy is utilized for quality assessment of agricultural products [6]. Nondestructive NIR methods have been used for predicting the quality of agricultural product such as soluble solid content (SSC) of Marian plum fruit [6]; soluble solids content in Nam Dok Mai mangoes [7], starch content, firmness, and acidity of Fuji apples [8], SSC of Rocha pears [9], and starch and DM content of fresh cassava tubers [10-13] Previous research confirmed that the assessment could be more accurate and reliable if the measurements were conducted using an appropriate methodology and if a suitable prediction model is developed.

Applying benchtop spectrometer NIR to measure the quality of durian pulp, Onsawai et al. [14] evaluated the DM of durian by scanning pulp and fruit, providing rough screening ability, with r^2 and RMSEP of 0.89 and 3.27%, respectively, using pulp spectra. The DM of the pulp could be reasonably predicted by scanning the intact durian fruit at the largest locule, with r^2 and RMSEP of 0.79 and 5.23%, respectively. Sharma et al. [15] applied NIR hyperspectral imaging coupled with various machine learning techniques, including partial least squares regression (PLSR), support vector machine (SVM), random forest (RF), and convolutional neural network (models: Custom, U-Net, VGG19), and variable selection methods, including genetic algorithm (GA) and successive projection algorithm (SPA), to evaluate the quality of durian pulp. GA and SPA achieved good results for DM ($r^2 = 0.97$) and FC ($r^2 = 0.86$). The GA-PLSR model was the best for predicting TSS, with an r^2 equal to 0.90, whereas the SPA-PLSR model provided poor performance, with an r^2 of 0.79. Ali et al. [16] applied a thermal imaging technique combined with multivariate analysis to predict the ripeness of durian fruit. PLSR results successfully developed quantitative prediction models with R^2 values exceeding 0.94. The SVM model achieved a classification accuracy of 97%, making it the most effective method for discriminating durian ripeness. This method requires temperature control of the sample and the testing room. Saechua et al. [17], studied the application of a Vis-SWNIR spectrometer integrated into a conveyor belt system in the production line to measure the DM of durian pulp, and the model was developed using PLSR, which was recommended to preprocess the spectra using a standard normal variate (SNV) to achieve R^2_P and RMSEP of 0.83, and 4.32%, respectively.

Measuring durian fruit remains challenging, and many researchers continue to investigate this topic. Phuangsombut et al. [18] predicted the DM of durian fruit with decreasing influence of spikes. Before scanning, the spikes were removed, and part of the rind of the most fertile locule of each fruit (approximately 2–3 mm thick) was sliced off to present a flat area. The prediction accuracy provided a coefficient of correlation of calibration (R^2_c) = 0.67 and root mean square error of cross-validation (RMSECV) = 2.68% [18]. However, this approach is not a completely nondestructive measurement. Ditcharoen et al. [19] developed a nondestructive model to classify the maturity stages (day after blooming [DAB]) of durian fruits by using long-wave NIR (LWNIR) and short-wave NIR (SWNIR), which was investigated by Ditcharoen et al. [19], and the spectra of durian fruit were collected while the fruit moved along a conveyor belt. Three algorithms—LDA, SVM, and KNN—were employed to estimate the three maturity stages. LWNIR achieved an accuracy of 83.15% to 88.04%, while SWNIR yielded an accuracy of 64.73% to 93.77%. This method could be used to screen the maturity stage of durian fruit using DAB. In the prediction models, the proportion of samples in each class directly influenced the classification accuracy. Issues such as class overlap and small sample sizes can hinder classifier learning [20]. Model accuracy was improved by generating synthetic samples using the synthetic minority oversampling technique (SMOTE) to balance the sample distribution. The SMOTE-based method not only addresses the issue of imbalanced sample distribution but also enhances the recognition accuracy of the classification model. Additionally, SMOTE was chosen to increase the sample size as it helps save time and reduces costs associated with oversampling [21]. Previous studies on durian DM prediction relied mainly on offline or DAB-based approaches, which are unsuitable for industrial use and are not directly linked to the export requirement of DM ≥ 32%. Such methods have limited robustness across orchards and seasons, and cannot support real-time quality control. Therefore, this study developed a nondestructive, online classification method for intact durians that directly targets the export threshold, providing a practical solution for implementation in production lines.

As noted in previous research, studies have focused on grading durian fruits by grouping them according to the number of DAB. However, research on classification based on DM content is limited. A key research gap is that predicting DAB can lead to errors, as durians of the same age (in DAB) may have different DM levels, which can result in grouping inaccuracies. Therefore, the objective of this study was to develop an NIR model to predict the quality of durian fruit as it moves along a conveyor belt. The sub-objectives of this study are twofold. First, it aims to evaluate the potential of online NIR spectroscopy for assessing durian fruit quality based on DM content, categorizing the fruit into two groups: rejected (DM < 32%) and accepted (DM ≥ 32%). Additionally, we investigated the performance of models developed with both imbalanced and balanced datasets using SMOTE to generate a balanced sample size, thus reducing the cost and effort associated with data collection for modeling. Second, it aims to predict the DM content of durian fruit by using PLSR. The outcomes of this study will help identify the most effective wavelengths (from both LWNIR and SWNIR), spectral preprocessing methods, and algorithms.

2. Materials and methods

2.1 Sample

This study used fresh durian (Monthong variety) samples collected from the Duang Kaen durian orchard in Nam Nao District, Phetchabun Province. A total of 130 samples were collected on five different DABs: 80–90 DAB (40 fruits, DM≈5.6–18.0%), 90–100 DAB (40 fruits, ≈ 18.1–29.6%), 100–110 DAB (20 fruits, ≈ 29.7–33.5%), 110–120 DAB (10 fruits, ≈ 33.6–38.0%), and 120–130 DAB (20 fruits, ≈ 38.1–43.5%). Sample collection was conducted by tracking the blooming date of each tree. The fruits were harvested once they reached the designated DAB range and were carefully transported to the laboratory. The room temperature was maintained at 25 °C.

A portion of the fruits at the premature stage were allowed to ripen at room temperature for 7 days prior to spectral scanning. These fruits were assigned to the ripe-stage group. Durian is a climacteric fruit that ripens after harvest and is regulated by ethylene production [22]. The imbalance in sample sizes occurred in DAB stages, with more samples collected at 80–100 DAB and fewer at 101–130 DAB owing to seasonal variation in flowering and fruit set. This imbalance affects model performance, particularly for DM classification.

This issue was addressed by using SMOTE to balance the minority class in the calibration set, whereas the test set remained unaltered to avoid overfitting.

2.2 Scanning

The online measurement system is illustrated in Figure 1. It included a conveyor, a measurement chamber, two NIR spectrometers, and a computer. Four 50 W halogen lamps were installed in the measurement chamber at each corner at 45° from the plane to serve as a light source. The halogen lamps were placed 50 cm from the conveyor belt, and the NIR spectrometers were positioned 15 cm away from the durian. The measurement chamber was a black box with dimensions of 60 × 60 × 60 cm. Each durian fruit was scanned on a conveyor while moving at a speed of 20 cm/s. An LWNIR spectrometer (AvaSpec-ULS2048-USB2-VA-50, AVANTES, the Netherlands) with a wavelength range of 860–1750 nm and an SWNIR spectrometer (AvaSpec-NIR256-1.7-EVO, AVANTES, Netherlands) with a wavelength range of 450– 1000 nm were used. The sample holder was fabricated from black material with a matte surface and rigid structure, providing stable support for the durian fruit during NIR measurements on the conveyor and minimizing light reflection and vibration interference.

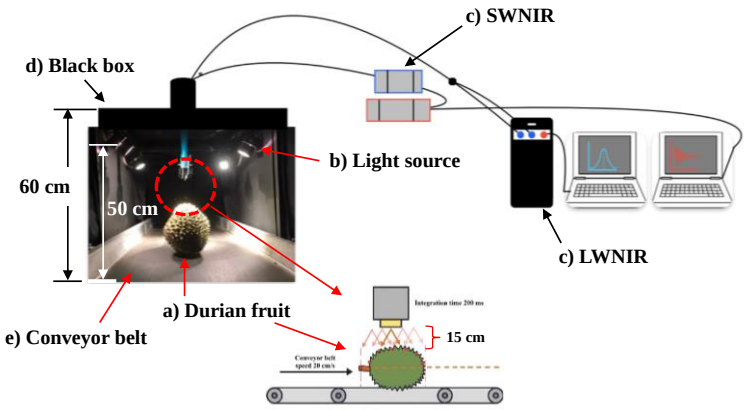

Figure 1 Scanning durian on a conveyor belt: a) durian fruit, b) light source, c) experimental equipment of online scanning (LWNIR and SWNIR), d) black box, and e) conveyor belt. (LWNIR: long-wavelengths near infrared; SWNIR: short-wavelengths near infrared)

Spectrum acquisition consisted of 3 steps: 1) The light source was switched on and allowed to stabilize for 10 min to ensure consistent light intensity. 2) Before the sample was scanned, a dark reference—an opaque black object—was used as a reference for background light reflection. We then set up a white reference, which serves as a reference for light reflection from a white opaque object. A material called spectralon reference was used, and the values were scanned to reduce other interfering factors, such as light or the use of a new machine. Scanning of the sample will yield a reflectance value between the dark (black) and white reference spectra. 3) The samples were scanned using two spectrometers with an integration time of 200 ms. Each fruit was scanned on the side corresponding to the main pulp (fertile lobe) as it passed beneath the light window, and the results were averaged [23]. The absolute reflection value was then obtained, and the relative reflectance was calculated as $R = \frac{R_s - R_d}{R_w - R_d}$, where R_s is the intensity of the reflected light of the sample (absolute reflectance), R_d is the dark reference, and R_w is the white reference. The spectral data were recorded as absorbance (A) = log(1/R), where R is the relative reflectance [24].

2.3 Uncertainty test of NIR spectra

This study investigated the accuracy and consistency of scanning durian pulp, focusing on factors such as measurement reliability, potential errors, and the effectiveness of the scanning method in capturing the physical and compositional characteristics of the pulp. The NIR spectra data of three durian fruits (sample nos. 5, 80, and 120) were used to calculate the uncertainty test of the NIR spectra. Three spectra were collected, as shown in Figure 2. Calculations were performed to verify the extent to which the spectrum values would differ if the same sample was scanned at three different positions, which served as a test for the uncertainty of future predictions. The root mean square (RMS) was reported as an indicator of the sample scanning precision and was calculated using the following formula:

$$RMS_j = \sqrt{\frac{\sum_{a=1}^{n}(X_{ab} - \bar{X}_a)^2}{n}} \quad (1)$$

where X_{ab} represents the absorption value of sample "a" at wavelength "b," $\bar{X}$ is the mean absorption value at wavelength "a" across all samples, and n is the total number of data points corresponding to the number of wavelengths. RMS_j denotes the RMS value for spectrum j. The RMS values were determined for the raw spectra, SNV, 1st derivative spectra, and 2nd derivative spectra. A low mean RMS value signifies high precision in the NIR data, indicating that the spectral measurements were highly consistent and exhibited minimal variation across repeated scans. This finding suggests that the NIR system is reliable for capturing the characteristics of durian pulp with little deviation. Conversely, a high mean RMS value suggests substantial differences between the individual spectra, even when scanning the same durian fruit. This implies low precision, as the variability in the spectral data may stem from inconsistencies in the scanning process, instrument sensitivity, or external factors that affect measurement stability.

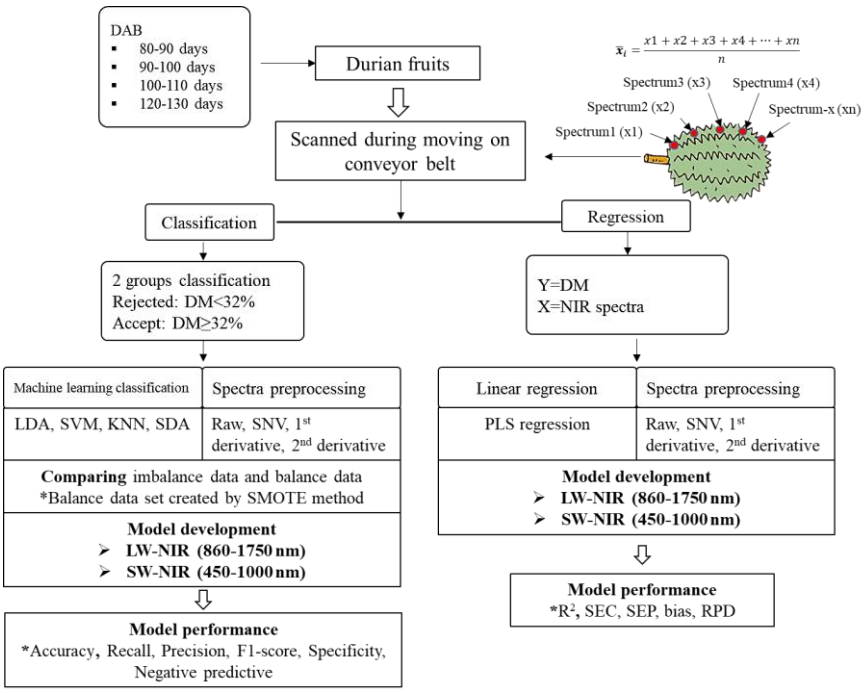

Figure 2 Flow diagrams for prediction model development of durian DM content for classifying quality (DAB: the durian at 5 different age stages after the flowers bloom)

2.4 Dry matter

After scanning, the fruit samples were peeled off. The durian pulp was used to determine the DM content. The pulp sample was divided into three parts: the head, middle, and tail. Each part was cut, weighed to 10 g, and placed in a hot-air oven at 60 ℃ for 48 h until a constant weight was achieved. DM was calculated using the following formula:

$$\text{Dry matter (\%)} = \frac{W_2}{W_1} \times 100 \quad (2)$$

where W_2 represents the final weight of the dried sample (g), and W_1 denotes the initial weight (g). Three replicates were averaged to obtain one, which was assigned as a representative DM [17, 19, 25]. Outliers in the measured DM were determined using the criterion $(y_i - \bar{y})/SD \geq \pm 3$, where y_i represents the DM value obtained from the reference method, $\bar{y}$ is the mean of the reference values, and SD is the standard deviation of the reference values. Any sample with a reference value that met this condition was excluded from the dataset.

2.5 Classification model

Durian fruit quality was categorized into two groups based on DM: accepted (DM ≥ 32%) and rejected (DM < 32%). Principal component analysis was performed on the raw spectral data to detect outliers. The process of developing the classification model is illustrated in Figure 2.

The classification model was developed based on three factors: 1) factors of different wavelength ranges: LWNIR and SWNIR; 2) factors of different algorithms: LDA, SVM, KNN, and ensemble SDA; and 3) factors of different spectral preprocessing: raw spectra, 1st derivative (segments = 5, gaps = 5), 2nd derivative (segments = 5, gaps = 5), and SNV. Therefore, 32 models or 32 treatments (2 wavelength ranges × 4 supervised algorithms × 4 spectral preprocessing) were derived. The dataset was split into 70% calibration set and 30% test set. SMOTE was applied only to the calibration set to avoid data leakage, while the model training used leave-one-out cross-validation (LOOCV). An independent test set containing only real samples was reserved for the final performance evaluation. The models were developed and evaluated using the test set method, maintaining a 3:1 ratio between calibration and validation sets. The robustness of the model was improved by using the SMOTE algorithm to increase the number of samples in the underrepresented group, making the sample size equal to that of the other group or ensuring that the sample groups were balanced. Subsequently, the model was constructed using the method described above. SMOTE is used to address class imbalance in datasets, particularly in machine learning. It generates synthetic samples for the minority class to balance the number of samples between the minority and majority classes [26].

The 1st derivative method helped alleviate the problem of increasing the spectral values across the wavelength (Y-axis), which caused the spectra to shift closer together. This adjustment ensured that the data were more accurate. The 2nd derivative separates the overlapping peak points in the spectrum and reduces the impact that causes the spectrum to increase in size throughout the range. The second derivative aligns the peak points with the original spectrum peaks even if they are inverted. SNV adjusts for the effects caused by light scattering, which often results in a multiplicative effect on absorbance values. Reducing the variability that leads to movement along the vertical axis of the spectrum helps correct for these effects [27].

LDA is a widely used technique for dimensionality reduction and classification. In this study, LDA is utilized to transform high-dimensional data into (n-1) components, where n is the total number of classes, by utilizing eigenvector decomposition. Additionally, LDA components are employed in conjunction with SVM, an algorithm that constructs hyperplanes or a set of hyperplanes in high-

dimensional or infinite-dimensional space. All points belonging to class A are designated as +1, whereas all points in class B are designated as -1 [28]. KNN utilizes a database in which data points are divided into several distinct classes to predict the classification of new sample points. This is considered one of the best-case scenarios demonstrated by the example [29]. This method utilizes an analysis technique from the k-nearest data points to the data that need to be classified by categorizing according to the majority class of the k-nearest training data points [16]. Ensembles are used to improve the predictive performance of modeling problems by combining multiple models instead of relying on a single model. This enhancement occurs because the ensemble approach reduces the variance component of the prediction error, albeit by introducing some bias [30]. The selection of SVM and RF as classification algorithms was supported by Wu et al. [31], who demonstrated that SVM achieved the highest accuracy and stability in spectral classification, whereas RF effectively reduced overfitting and provided insights into feature importance.

The performance of the model was evaluated using several metrics, including accuracy (Eq. 3), precision (Eq. 4), recall (Eq. 5), specificity (Eq. 6), and F1-score (Eq. 7). These equations are based on four key variables: true positives (TP), true negatives (TN), false positives (FP), and false negatives (FN). It is calculated using the following formula:

$$\text{Overall accuracy} = \frac{TP+TN}{TP+TN+FP+FN} \times 100 \quad (3)$$

$$\text{Precision} = \frac{TP}{TP+FP} \times 100 \quad (4)$$

$$\text{Recall} = \frac{TP}{TP+FN} \times 100 \quad (5)$$

$$\text{Specificity} = \frac{TN}{TN+FP} \times 100 \quad (6)$$

$$\text{F1-Score} = 2 \times \frac{\text{Precision} \times \text{Recall}}{\text{Precision} + \text{Recall}} \quad (7)$$

The overall accuracy indicates the model's performance when immature durians are predicted to be mature and mature durians are predicted as another group. Precision indicates the performance of the model when the prediction result is FP, where immature durians are predicted to be mature. Recall indicates the performance of the model when the prediction result is FN, where mature durians are predicted as another group. Specificity indicates the model's performance when the prediction result is TP, where mature durians are predicted as another group [32].

2.6 Predictive regression model

A flowchart illustrating the model development for durian fruit at various stages of maturity using an online NIR spectroscopy system is shown in Figure 2. The DM model was developed through PLSR considering different factors, such as the use of various spectral pretreatment methods (four treatments: raw, first derivative, second derivative, and SNV), and factors of different wavelength ranges (two treatments: LWNIR and SWNIR). A total of 12 treatments ($2 \times 8 = 12$) were analyzed. Each treatment was applied to the calibration and validation sets with a separation ratio of 3:1 between the two sets. For regression models, SMOTE was not applied because regression requires continuous target values, and no class imbalance adjustment is necessary. In both cases, the calibration and test sets were independent, non-overlapping, and randomly selected to avoid bias and ensure a fair model evaluation. Model evaluation was performed using LOOCV. In this approach, a single sample is set aside as the test set in each iteration, whereas all the remaining samples are used to train the model. This process was repeated until every sample was used exactly once for validation. This method is particularly suitable for datasets with limited sample sizes because it maximizes data utilization and provides a reliable estimate of model performance.

Once the models were created, they were validated using a prediction set. Model performance was evaluated based on several statistical parameters, including the coefficient of determination (R^2), standard error of calibration (SEC), standard error of prediction (SEP), ratio of prediction to standard deviation (RPD), and bias. According to commonly accepted criteria, good model performance was indicated by $R^2 > 0.90$ and $RPD > 3$ [33].

3. Results and discussion

3.1 NIR spectra

The durian spectra collected by scanning on conveyor belts at different wavelength ranges, namely, LWNIR (860–1750 nm) and SWNIR (450–1000 nm), are illustrated in Figures 3 and 4. Figure 3 illustrates the spectra of whole durian fruit versus the black conveyor belt for LWNIR and SWNIR, where the absorption of the conveyor is higher than that of durian fruit. The advantage is that it makes it easier to distinguish between the spectra of durian and non-durian objects, which helps the online measurement system easily identify durian fruit. Figure 4 shows the NIR spectra collected from the LWNIR and SWNIR spectrometers, which were either raw spectra or preprocessed by SNV, 1st derivative and 2nd derivative, respectively. Figure 4 also shows the spectra based on two groups: rejected group (DM < 32%: red line) and accepted group (DM ≥ 32%: blue line). In the raw spectra, the distinction between the two sample groups was not very clear compared with the spectra that were processed. An obvious absorption peak was found at wavelengths of 681 and 1450, corresponding to the absorption bands of anthocyanins and chlorophylls [34], vibration of the third overtone of O-H stretches [35], and water content, which is the vibrational band of H_2O [35]. The spectral variation observed in the peel reflects compositional changes associated with fruit maturation, particularly an increase in pulp DM and a corresponding decrease in peel moisture. This chemical relationship between the peel and pulp enables the use of peel spectra as an indirect indicator for predicting internal pulp quality [36, 37]. Distinct differences in the absorbance values at each maturity stage were observed. The absorbance values varied across different DM. As mentioned earlier, these distinct differences in absorbance values across different maturity stages make the model efficient for accurately classifying groups [38].

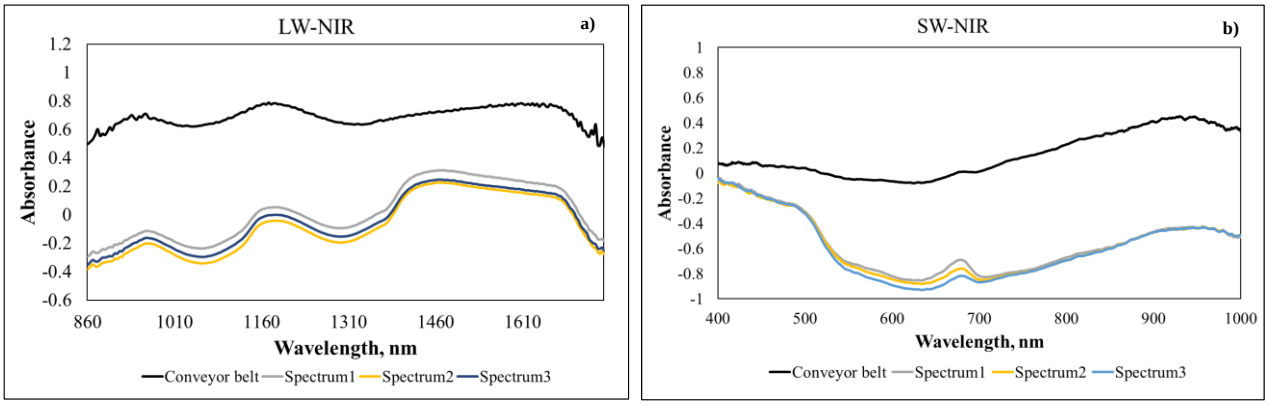

Figure 3 Spectra of durian fruit vs. conveyor belt, a) LWNIR and b) SWNIR

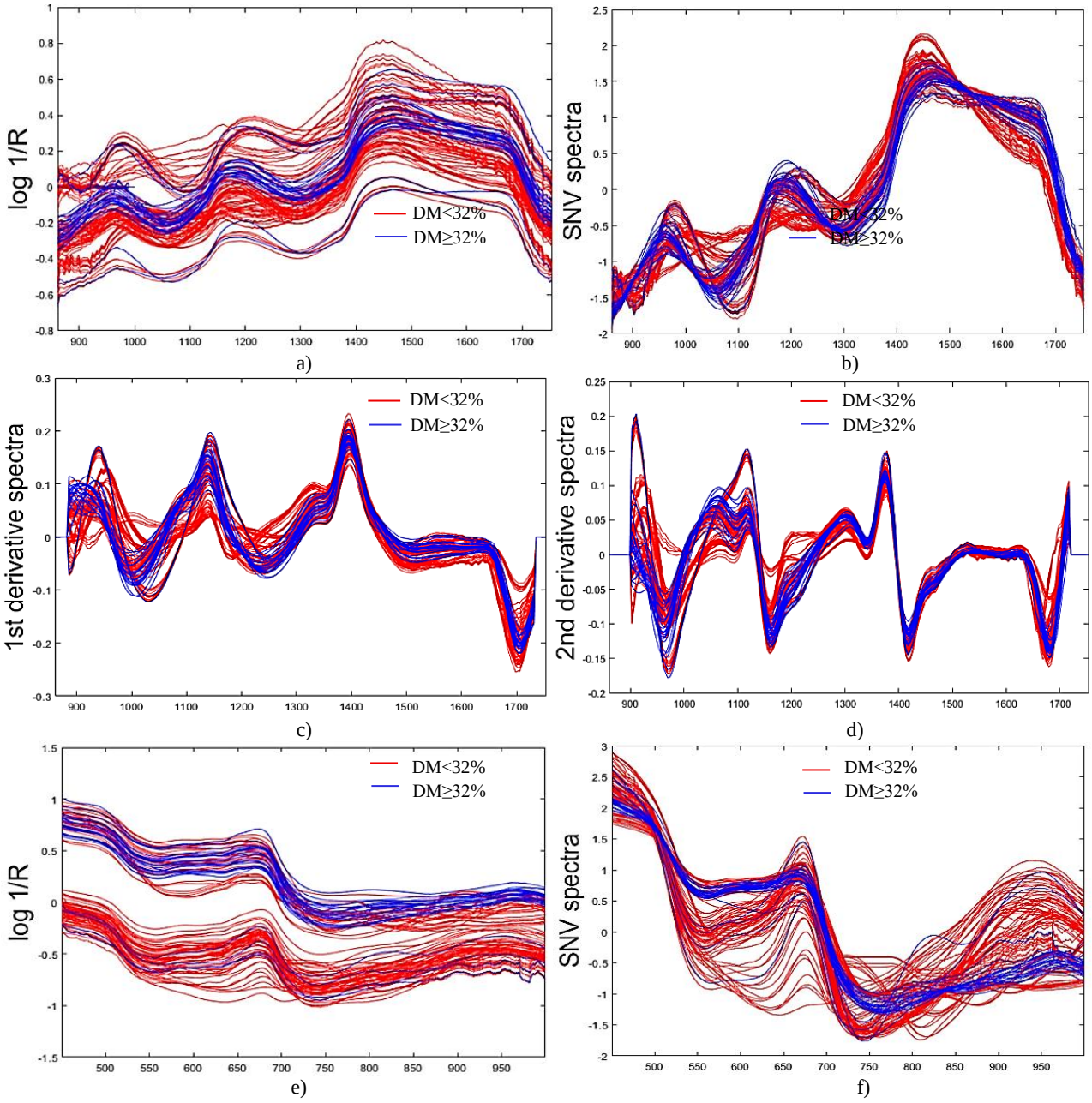

Figure 4 Spectra of durian fruit, a) LWNIR as raw spectra, b) LWNIR as SNV spectra, c) LWNIR as 1st derivative spectra, d) LWNIR as 2nd derivative spectra, e) SWNIR as raw spectra, f) SWNIR as SNV spectra, h) SWNIR as 1st derivative spectra, and i) SWNIR as 2nd derivative spectra.

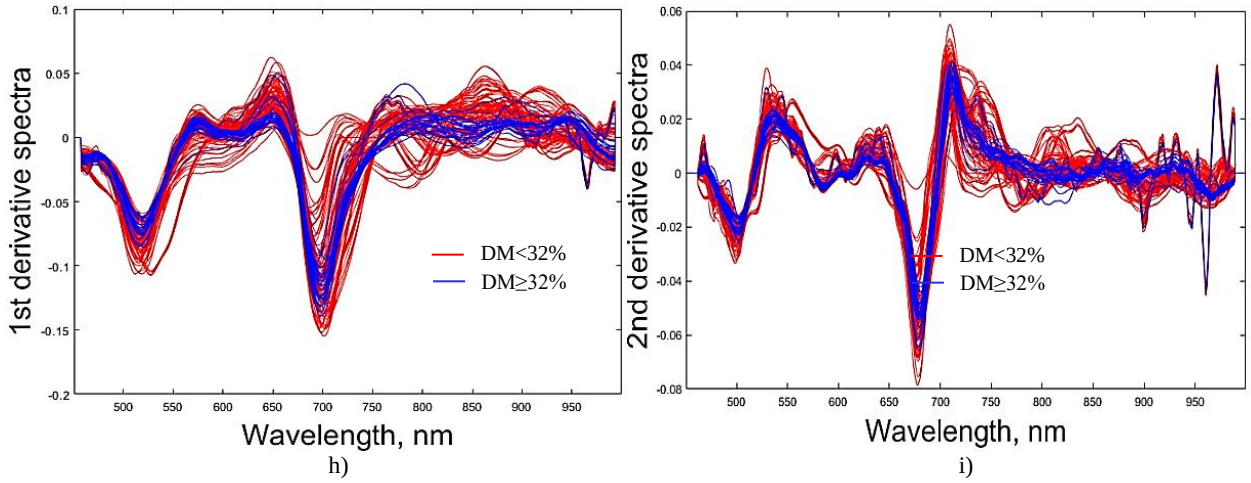

h) i)

Figure 4 (continued) Spectra of durian fruit, a) LWNIR as raw spectra, b) LWNIR as SNV spectra, c) LWNIR as 1st derivative spectra, d) LWNIR as 2nd derivative spectra, e) SWNIR as raw spectra, f) SWNIR as SNV spectra, h) SWNIR as 1st derivative spectra, and i) SWNIR as 2nd derivative spectra.

Table 1 RMS value of sample nos. 5, 80, and 120 calculated from raw spectra.

Sample no.		LWNIR				SWNIR			
		RMS_1	**RMS_2**	**RMS_3**	**$\overline{RMS}$**	**RMS_1**	**RMS_2**	**RMS_3**	**$\overline{RMS}$**
5	Raw	0.007538	0.010675	0.017617	0.01194	0.128222	0.115193	0.24307	0.16216
	1st derivative	0.002295	0.002086	0.004004	0.00280	0.008897	0.005359	0.013204	0.00915
	2nd derivative	0.002221	0.001968	0.003683	0.00262	0.007467	0.005238	0.010366	0.00769
	SNV	0.009382	0.012336	0.017814	0.01318	0.165556	0.130693	0.28743	0.19456
80	Raw	0.095774	0.051651	0.044186	0.06387	0.024203	0.00578	0.025647	0.01854
	1st derivative	0.006056	0.002695	0.003821	0.00419	0.004846	0.002335	0.004695	0.00396
	2nd derivative	0.005855	0.002126	0.004059	0.00401	0.004546	0.003268	0.004522	0.00411
	SNV	0.048778	0.023742	0.026362	0.03296	0.066832	0.027757	0.069259	0.05462
120	Raw	0.014819	0.01700	0.029648	0.02049	0.077863	0.018479	0.070431	0.05559
	1st derivative	0.005446	0.002372	0.007742	0.00519	0.010688	0.008712	0.009326	0.00958
	2nd derivative	0.003929	0.001828	0.00561	0.00379	0.016238	0.013914	0.01359	0.01458
	SNV	0.035926	0.011984	0.046738	0.03155	0.129225	0.086665	0.13023	0.11537

Table 1 reports the RMS value of durian fruit (samples no. 5, 80, and 120) calculated from the raw spectra. RMS value is a measure of the precision of the NIR spectrometer to produce consistent absorption values when measuring the same durian sample multiple times. Therefore, if the RMS value is low, then the absorption values for the same durian sample are close to each other when measured repeatedly [39]. However, if the RMS value is high, then the absorption values for the same sample vary significantly across repeated measurements.

The experimental results show that LWNIR provides a lower RMS value than SWNIR, which could be because the LWNIR range allows the detector to be less affected by external light interference. However, both wavelength ranges had RMS values of no more than approximately 0.1. When comparing these RMS with the relative absorption values, which range from 0 to 1, the obtained RMS values are relatively low and acceptable for model development.

3.2 Dry matter

Table 2 shows the average DM values of durian flesh, categorized based on DM weight into two groups: those with DM < 32% and those with DM ≥ 32%. This categorization was based on the standard set by the Department of Agriculture and Food Product Standards [4], which defines durians with a DM ≥ 32% as suitable for harvesting, indicating good maturity. This finding shows that the DM value correlates with durian maturity. After outlier detection, the outliers of 18 samples were met and removed from the dataset. In the model experiment, the data were divided into calibration and validation sets. The division ratio was 3:1, with 87 samples in the calibration set and 25 samples in the validation set, which were randomly selected. Arranged from highest to lowest, the samples with the highest and lowest values were placed in the calibration set, which includes maximum, minimum, average, and SD.

Table 2 Statistical value of the DM content of durian fruit sample.

Data set	N	Max	Min	Mean	SD
Calibration set	87	43.52	5.61	20.80	11.85
Validation set	25	41.87	6.59	20.64	11.46
DM < 32% group	25	29.60	5.61	15.44	6.74
DM ≥ 32% group	87	43.52	33.57	39.91	2.41

Notes: [N] Number of samples; [Max] Maximum; [Min] Minimum; [SD] Standard deviation

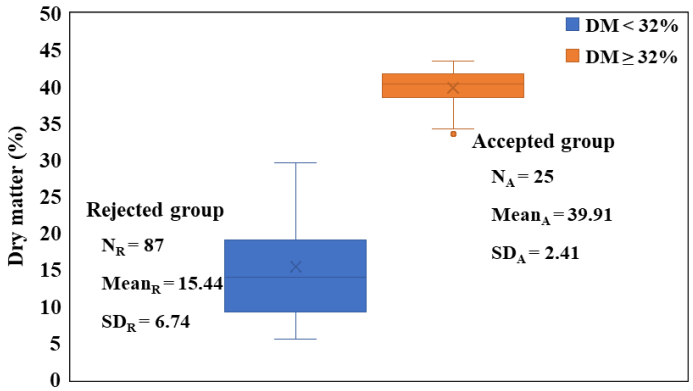

Figure 5 Box plot of DM distribution in durian between the rejected group (DM < 32%) and the accepted group (DM ≥ 32%).

The box plot demonstrated that the rejected group (DM < 32%) exhibited a lower mean DM content (15.44%) with high variability (SD = 6.74), indicating inconsistent fruit quality. By contrast, the accepted group (DM ≥32%) showed a higher mean DM (39.91%) with lower variability (SD = 2.41), reflecting a more uniform quality that met export standards. The clear separation between these groups supports the use of the DM ≥ 32% threshold as a reliable criterion for durian quality classification (see Figure 5).

3.3 Classification model

3.3.1 Model evaluation on imbalanced data

The models were built to classify durian maturity using LWNIR spectra with wavelengths ranging from 860 to 1750 nm (LWNIR) and 450 to 1000 nm (SWNIR spectra). The modeling process involved different factors, namely, different algorithms (LDA, SVM, KNN, and SDA), and different spectral preprocessing methods (raw, SNV, 1st derivative, and 2nd derivative). The models were developed from an imbalanced sample and improved using a balanced dataset created using the SMOTE method. Then, the performance of the models was calculated based on confusion metrics such as overall accuracy, recall, precision, F1-score, specificity, and negative predictive value, which were calculated based on the frequency from the confusion matrix of the classification model (see Figure 6).

	Actually Positive (1)	Actually Negative (2)	
Predicted Positive (1)	True Positive (TP)	False Positive (FP)	**Positive Predictive** $= \frac{TP}{TP + FP} \times 100$
Predicted Negative (2)	False Negative (FN)	True Negative (TN)	**Negative Predictive** $= \frac{TN}{TN + FN} \times 100$
	Recall $= \frac{TP}{TP + FN} \times 100$	**Specificity** $= \frac{TN}{TN + FP} \times 100$	**Accuracy** $= \frac{TP+TN}{TP+TN+FP+FN} \times 100$

Figure 6 Confusion matrix of model frequency for conveyor scanning of calibration set and validation set.

Table 3 presents the performance of the classification model developed using LWNIR coupled with different methods. This consisted of the results of the calibration and test sets. For the imbalanced dataset, the model developed from the raw spectra showed low ability. Meanwhile, the SNV-KNN, 1st derivative-LDA, 1st derivative-KNN, and 2nd derivative-KNN models provided highly effective prediction results. Although the number of samples between the two groups was imbalanced, the prediction outcomes helped minimize the impact on recall, precision, and F1-score values. The 1st derivative-LDA model provides the best performance both in the calibration set and test sets.

3.3.2 Performance improvement after SMOTE balancing

The results of improving the model by creating a balanced dataset clearly showed that the model's performance in both the calibration and test sets significantly increased the recall, precision, and F1-score, leading to a noticeable improvement in the overall performance of the model. For our results, the model developed using the 1st derivative-LDA still provided effective performance, accuracy, recall, precision, F1-score, specificity, and negative predictive values of 0.95, 1.00, 0.90, 0.95, 0.91, and 1.00, respectively. The overall results for the test set are shown in Figures 7a and 7b.

Table 4 shows the performance of the classification model developed using SWNIR in combination with various methods. It includes results from both the calibration set and the test set. For the model developed from the imbalanced samples, a significant issue with low recall, precision, and F1-score was observed as a result of the imbalance in the number of samples between the groups. After the model was improved by creating new data to balance the two datasets, its performance improved significantly (Figures 7c and 7d). Evidently, the recall, precision, and F1-score values increased substantially. The results show that the performance of all models improved. The model is highly efficient, and there is not much noticeable difference. In the researcher's opinion, the 2nd derivative-SVM model provides effective performance, with accuracy, recall, precision, F1-score, specificity, and negative predictive values of 0.88, 0.84, 0.89, 0.86, 0.91 and 0.87, respectively.

Table 3 Classification result of the validation set of durians at two different grade levels using various multivariate algorithms and spectra data obtained from LWNIR

		Calibration set										Test set					
Imbalanced samples		**TP**	**FN**	**TN**	**FP**	**Accuracy**	**Recall**	**Precision**	**F1-score**	**Specificity**	**Negative predictive**	**Accuracy**	**Recall**	**Precision**	**F1-score**	**Specificity**	**Negative predictive**
Raw	LDA	15	4	64	3	0.92	0.79	0.83	0.81	0.96	0.94	0.83	0.67	0.57	0.62	0.87	0.91
	SVM	0	19	67	0	0.78	0.00	0.00	0.00	1.00	0.78	0.79	0.00	0.00	0.00	1.00	0.79
	KNN	16	3	55	12	0.83	0.84	0.57	0.68	0.82	0.95	0.79	0.33	0.50	0.40	0.91	0.84
	SDA	16	3	64	3	0.93	0.84	0.84	0.84	0.96	0.96	0.83	0.67	0.57	0.62	0.87	0.91
SNV	LDA	17	2	60	7	0.90	0.89	0.71	0.79	0.90	0.97	0.83	0.67	0.57	0.62	0.87	0.91
	SVM	8	11	65	2	0.85	0.42	0.80	0.55	0.97	0.86	0.83	0.50	0.60	0.55	0.91	0.88
	KNN	***16***	***2***	***63***	***4***	***0.93***	***0.89***	***0.80***	***0.84***	***0.94***	***0.97***	***0.90***	***0.83***	***0.71***	***0.77***	***0.91***	***0.95***
	SDA	16	3	60	7	0.88	0.84	0.70	0.76	0.90	0.95	0.83	0.67	0.57	0.62	0.87	0.91
1st_dev	**LDA**	**14**	**5**	**62**	**5**	**0.88**	**0.74**	**0.74**	**0.74**	**0.93**	**0.93**	**0.95**	**1.00**	**0.90**	**0.95**	**0.91**	**1.00**
	SVM	12	7	65	2	0.90	0.63	0.86	0.73	0.97	0.90	0.86	0.67	0.67	0.67	0.91	0.91
	KNN	***17***	***2***	***63***	***4***	***0.93***	***0.89***	***0.81***	***0.85***	***0.94***	***0.97***	***0.93***	***0.83***	***0.83***	***0.83***	***0.96***	***0.96***
	SDA	14	5	63	4	0.90	0.74	0.78	0.76	0.94	0.93	0.83	0.67	0.57	0.62	0.87	0.91
2nd_dev	LDA	16	3	61	6	0.90	0.84	0.73	0.78	0.91	0.95	0.79	0.67	0.50	0.57	0.83	0.90
	SVM	13	6	66	1	0.92	0.68	0.93	0.79	0.99	0.92	0.83	0.50	0.60	0.55	0.91	0.88
	KNN	***17***	***2***	***63***	***4***	***0.93***	***0.89***	***0.81***	***0.85***	***0.94***	***0.97***	***0.93***	***0.83***	***0.83***	***0.83***	***0.96***	***0.96***
	SDA	15	4	64	3	0.92	0.79	0.83	0.81	0.96	0.94	0.83	0.67	0.57	0.62	0.87	0.91
Balanced samples		**TP**	**FN**	**TN**	**FP**	**Accuracy**	**Recall**	**Precision**	**F1-score**	**Specificity**	**Negative predictive**	**Accuracy**	**Recall**	**Precision**	**F1-score**	**Specificity**	**Negative predictive**
Raw	LDA	56	0	59	8	0.93	1.00	0.88	0.93	0.88	1.00	0.93	1.00	0.86	0.93	0.87	1.00
	SVM	50	6	45	22	0.77	0.89	0.69	0.78	0.67	0.88	0.74	0.84	0.67	0.74	0.65	0.83
	KNN	51	5	63	4	0.93	0.91	0.93	0.92	0.94	0.93	0.88	0.89	0.85	0.87	0.87	0.91
	SDA	52	2	60	7	0.93	0.96	0.88	0.92	0.90	0.97	0.90	1.00	0.83	0.90	0.83	1.00
SNV	LDA	56	0	62	5	0.96	1.00	0.92	0.96	0.93	1.00	0.93	1.00	0.86	0.93	0.87	1.00
	SVM	47	9	59	8	0.86	0.84	0.85	0.85	0.88	0.87	0.81	0.74	0.82	0.78	0.87	0.80
	KNN	55	1	59	8	0.93	0.98	0.87	0.92	0.88	0.98	0.88	0.95	0.82	0.88	0.83	0.95
	SDA	56	0	64	3	0.98	1.00	0.95	0.97	0.96	1.00	0.90	1.00	0.83	0.90	0.83	1.00
1st_dev	LDA	56	0	55	12	0.90	1.00	0.82	0.90	0.82	1.00	**0.95**	1.00	0.90	0.95	0.91	1.00
	SVM	45	11	61	6	0.86	0.80	0.88	0.84	0.91	0.85	0.83	0.74	0.88	0.80	0.91	0.81
	KNN	50	5	63	4	0.93	0.91	0.93	0.92	0.94	0.93	0.93	0.95	0.90	0.92	0.91	0.95
	SDA	54	2	58	9	0.91	0.96	0.86	0.91	0.87	0.97	**0.93**	1.00	0.86	0.93	0.87	1.00
2nd_dev	LDA	56	0	54	13	0.89	1.00	0.81	0.90	0.81	1.00	0.93	1.00	0.86	0.93	0.87	1.00
	SVM	49	7	63	4	0.91	0.88	0.92	0.90	0.94	0.90	**0.90**	0.89	0.89	0.89	0.91	0.91
	KNN	54	2	62	5	0.94	0.96	0.92	0.94	0.93	0.97	0.90	0.95	0.86	0.90	0.87	0.95
	SDA	56	0	54	13	0.89	1.00	0.81	0.90	0.81	1.00	**0.90**	1.00	0.83	0.90	0.83	1.00

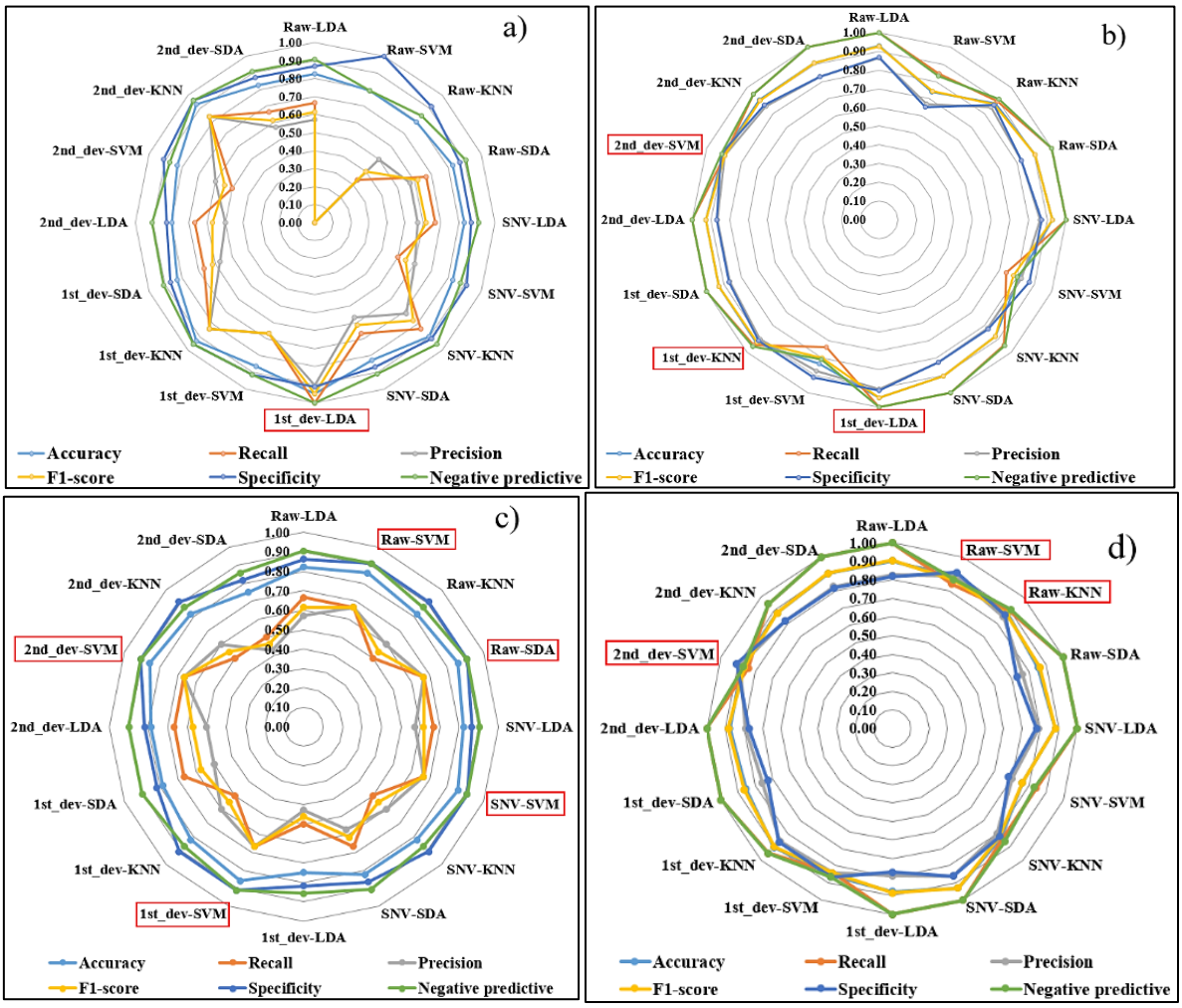

Figure 7 Performance of classification model as test set developed using a) LWNIR developed by imbalanced samples b) LWNIR developed by balanced samples c) SWNIR developed by imbalance samples and d) SWNIR developed by balanced samples

Table 4 Classification result of the validation set of durians at two different grade levels using various multivariate algorithms and spectra data obtained from SWNIR

		Calibration set										Test set					
Imbalanced sample		**TP**	**FN**	**TN**	**FP**	**Accuracy**	**Recall**	**Precision**	**F1-score**	**Specificity**	**Negative predictive**	**Accuracy**	**Recall**	**Precision**	**F1-score**	**Specificity**	**Negative predictive**
Raw	LDA	17	2	65	3	0.94	0.89	0.85	0.87	0.96	0.97	0.82	0.67	0.57	0.62	0.86	0.90
	SVM	17	2	64	4	0.93	0.89	0.81	0.85	0.94	0.97	0.86	0.67	0.67	0.67	0.91	0.91
	KNN	14	5	63	5	0.89	0.74	0.74	0.74	0.93	0.93	0.82	0.50	0.60	0.55	0.91	0.87
	SDA	17	2	64	4	0.93	0.89	0.81	0.85	0.94	0.97	0.86	0.67	0.67	0.67	0.91	0.91
SNV	LDA	17	2	66	2	0.95	0.89	0.89	0.89	0.97	0.97	0.82	0.67	0.57	0.62	0.86	0.90
	SVM	5	14	67	1	0.83	0.26	0.83	0.40	0.99	0.83	0.86	0.67	0.67	0.67	0.91	0.91
	KNN	16	3	60	8	0.87	0.84	0.67	0.74	0.88	0.95	0.82	0.50	0.60	0.55	0.91	0.87
	SDA	17	2	63	5	0.92	0.89	0.77	0.83	0.93	0.97	0.82	0.67	0.57	0.62	0.86	0.90
1st_dev	LDA	15	4	63	5	0.90	0.79	0.75	0.77	0.93	0.94	0.75	0.50	0.43	0.46	0.82	0.86
	SVM	15	4	66	2	0.93	0.79	0.88	0.83	0.97	0.94	0.86	0.67	0.67	0.67	0.91	0.91
	KNN	15	4	64	4	0.91	0.79	0.79	0.79	0.94	0.94	0.82	0.50	0.60	0.55	0.91	0.87
	SDA	11	8	61	7	0.83	0.58	0.61	0.59	0.90	0.88	0.79	0.67	0.50	0.57	0.82	0.90
2nd_dev	LDA	12	7	62	6	0.85	0.63	0.67	0.65	0.91	0.90	0.79	0.67	0.50	0.57	0.82	0.90
	SVM	16	3	66	2	0.94	0.84	0.89	0.86	0.97	0.96	0.86	0.67	0.67	0.67	0.91	0.91
	KNN	12	7	63	5	0.86	0.63	0.71	0.67	0.93	0.90	0.82	0.50	0.60	0.55	0.91	0.87
	SDA	16	3	63	5	0.91	0.84	0.76	0.80	0.93	0.95	0.75	0.50	0.43	0.46	0.82	0.86
Balance sample		**TP**	**FN**	**TN**	**FP**	**Accuracy**	**recall**	**precision**	**F1-score**	**Specificity**	**Negative predictive**	**Accuracy**	**Recall**	**Precision**	**F1-score**	**Specificity**	**Negative predictive**
Raw	LDA	54	2	64	4	0.95	0.96	0.93	0.95	0.94	0.97	0.90	1.00	0.83	0.90	0.82	1.00
	SVM	47	9	63	5	0.89	0.84	0.90	0.87	0.93	0.88	0.88	0.84	0.89	0.86	0.91	0.87
	KNN	52	4	58	10	0.89	0.93	0.84	0.88	0.85	0.94	0.88	0.89	0.85	0.87	0.86	0.90
	SDA	54	2	56	12	0.89	0.96	0.82	0.89	0.82	0.97	0.85	1.00	0.76	0.86	0.73	1.00
SNV	LDA	56	0	61	17	0.87	1.00	0.77	0.87	0.78	1.00	0.88	1.00	0.79	0.88	0.78	1.00
	SVM	47	9	51	17	0.79	0.84	0.73	0.78	0.75	0.85	0.76	0.84	0.70	0.76	0.68	0.83
	KNN	53	3	61	7	0.92	0.95	0.88	0.91	0.90	0.95	0.83	0.84	0.80	0.82	0.82	0.86
	SDA	56	0	57	11	0.91	1.00	0.84	0.91	0.84	1.00	0.93	1.00	0.86	0.93	0.86	1.00
1st_dev	LDA	54	2	60	8	0.92	0.96	0.87	0.92	0.88	0.97	0.88	1.00	0.79	0.88	0.77	1.00
	SVM	47	9	59	9	0.85	0.84	0.84	0.84	0.87	0.87	0.85	0.84	0.84	0.84	0.86	0.86
	KNN	54	2	55	13	0.88	0.96	0.81	0.88	0.81	0.96	0.90	0.95	0.86	0.90	0.86	0.95
	SDA	54	2	50	18	0.84	0.96	0.75	0.84	0.74	0.96	0.85	1.00	0.76	0.86	0.73	1.00
2nd_dev	LDA	56	0	57	11	0.91	1.00	0.84	0.91	0.84	1.00	0.88	1.00	0.79	0.88	0.77	1.00
	SVM	**48**	**8**	**62**	**6**	**0.89**	**0.86**	**0.89**	**0.87**	**0.91**	**0.89**	**0.88**	**0.84**	**0.89**	**0.86**	**0.91**	**0.87**
	KNN	56	0	58	10	0.92	1.00	0.85	0.92	0.85	1.00	0.88	0.95	0.82	0.88	0.82	0.95
	SDA	56	0	46	22	0.82	1.00	0.72	0.84	0.68	1.00	0.90	1.00	0.83	0.90	0.82	1.00

3.3.3 Comparison between LWNIR and SWNIR

A comparison of the model performance between LWNIR and SWNIR shows that the classification model built using the LWNIR wavelength range performed significantly better than that built using SWNIR, particularly when the samples between the two groups were imbalanced. However, when the two groups were balanced, the performance of both LWNIR and SWNIR was similar. Thus, both wavelengths could be used for online measurement. In addition, the LDA and KNN algorithms, when combined with derivative-based spectral preprocessing, performed well for both LWNIR and SWNIR. This result could be attributed to the fact that the LWNIR range has a higher absorbance and is less susceptible to external light interference compared with the SWNIR range. Additionally, the experimental results from both wavelength ranges indicated that scanning along the entire length of the durian fruit to obtain a spectrum representative of the whole fruit helped reduce the impact of spikes more effectively than scanning individual points, as reported in previous studies. This approach resulted in a more efficient model. However, some areas still require further investigation. For instance, increasing the intensity of the light source may improve the prediction accuracy because it can help reduce the scanning noise and enhance the overall performance. The performance of the 1st derivative and LDA models can be attributed to the reduced baseline drift and improved class separation, enhancing the classification accuracy. While we acknowledge trade-offs between accuracy and precision across models, simpler approaches, such as LDA, with fewer latent variables, offer practical advantages for real-time application. This finding is consistent with Cen and He [40], who showed that derivative preprocessing combined with linear classifiers improves online interpretability and efficiency [40]. LWNIR (860–1750 nm) has a wavelength range that covers more than that of SWNIR (450–1000 nm). The absorption bands are related to the water and starch components (e.g., the region around 1450 nm, which corresponds to the DM value), which play a crucial role in determining the ripeness levels of durian. As a result, the LWNIR model has significantly higher accuracy in cases of imbalanced data. After the application of SMOTE, the performance gap between LWNIR and SWNIR diminished, indicating that the initial superiority of LWNIR was mainly due to class imbalance rather than inherent spectral advantages.

The use of SMOTE effectively addresses the problem of class imbalance by generating additional samples for minority classes, enabling the model to learn more comprehensively and improving performance metrics, such as F1-score and balanced accuracy. However, synthetic data generation may introduce noise or lead to overfitting if applied inappropriately, and the outcomes largely depend on dataset characteristics and classifier sensitivity. Therefore, selecting the appropriate SMOTE variant is crucial to ensure optimal results for a given dataset and model. [26, 41].

Our results showed similar accuracy to the experiment by Talabnark and Terdwongworakul [42], in which durian fruits were scanned while stationary. They found that FT-NIR across the full wavelength range (800–2500 nm) could classify the maturity levels of durian fruit at different ages (101, 108, 115, and 122 DAB), using smoothed peel spectra with a reasonably high accuracy of 87.48%. Somton et al. [37] also reported a classification model developed using NIR (1000–2500 nm) [37]. Their model, which combined peel and stem spectra from stationary scans, achieved a higher accuracy than that based solely on peel spectra, reaching 94.4% compared with 87.5%. This result demonstrated that incorporating spectra from durian stems along with peel spectra improved classification accuracy. By contrast, Timkhum and Terdwongworakul [43] used SWNIR (350–750 nm) to distinguish between five ripening stages (106–134 DAB) of durian fruits, with a classification accuracy of 83.30%. These findings are consistent with previous analyses that compared short- and long-wave spectra, suggesting that models that use different wavelength ranges perform similarly in classification tasks.

3.4 Regression model

The results of the regression models are shown in Table 5, which presents the prediction results for DM developed using LWNIR and SWNIR spectra with R^2, SEP, RPD, and bias values. The analysis showed that for LWNIR spectral analysis, the second derivative method performed the best, with calibration (R^2c) values of 0.85 and validation (R^2v) values of 0.89. The standard errors of calibration (SEC), cross-validation (SECV), and prediction (SEP) were 4.75%, 6.23%, and 5.00%, respectively, and the RPD was 2.29. For SWNIR spectral analysis, the raw spectra provided the highest accuracy, with R^2c for the calibration set being 0.83 and R^2v for the validation set being 0.80. SEC, SECV, and SEP were 11%, 4.37%, and 6.69%, respectively, with an RPD of 1.71. The scatter plot compares the measured and predicted values from PLSR, as shown in Figure 8. Although the SW-raw model achieved high accuracy, the SW-2nd derivative model was considered more practical for real-time applications. This is because the 2nd derivative not only reduced the number of required latent variables, thereby improving model simplicity and minimizing the risk of overfitting, but also corrected for baseline shifts and light scattering while enhancing the resolution of overlapping peaks. These advantages lead to more robust and interpretable models, which are crucial for reliable implementation of online NIR spectroscopy systems. The model that uses spectra from LWNIR with 2nd derivative processing shows the highest efficiency in predicting the durian DM value. This is because LWNIR covers the absorption bands of water and starch. In particular, the region of 1450 nm corresponds to the O–H stretching overtone that reflects the moisture content and DM well (see Figure 9). Using the 2nd derivative, it also helps reduce scatter noise and baseline from the durian peel and allows the model to differentiate samples more accurately. However, the models were developed for specific orchards and varieties, which may introduce bias when applied to other cultivation areas. Therefore, external validation across different orchards and cultivars is recommended prior to large-scale industrial adoption.

Our research demonstrated better performance than Phuangsombut et al. [18] and Onsawai et al. [14] did in creating models to predict the DM content of durian. Our research achieved an R^2 of 0.89, while Phuangsombut et al. [18] obtained an R^2 of 0.67 and Onsawai et al. [14] achieved an R^2 of 0.55 [13,17]. Which is consistent with Puttipipatkajorn et al. [44], who showed that the rind and stem spectra can indirectly predict durian pulp DM. Unlike their offline setup, this study developed an online NIR system that can classify intact fruits on a conveyor, demonstrating practical applicability for industrial use. The strong LWNIR absorption around 1450 nm further confirmed the physiological linkage between the rind and pulp, supporting real-time maturity assessment [44]. Our study used an online spectral measurement method that involved measuring the spectra of the entire fruit, representing the entire durian. By contrast, previous studies employed point-based contact scanning with or without removing the spikes, which had a significant impact on the spectra.

Table 5 Results of modeling for DM weight prediction for conveyor belt scanning data of LWNIR and SWNIR

Spectral range	Calibration set						Validation set				
	Pretreatment	N	Factor	R^2_c	SEC	SECV	n	R^2_v	SEP	RPD	Bias
LW	Raw	87	10	0.78	5.51	6.76	25	0.81	6.45	1.78	-0.14
	1st_dev		12	0.81	5.07	6.79		0.85	5.70	2.01	0.43
	2nd_dev		**12**	**0.85**	**4.75**	**6.23**		**0.89**	**5.00**	**2.29**	-0.05
	SNV		13	0.79	5.38	7.08		0.83	6.09	1.88	0.04
SW	Raw	87	11	0.85	4.37	6.25	25	0.80	6.69	1.71	-0.17
	1st_dev		6	0.80	5.18	6.26		0.77	7.15	1.60	-0.17
	2nd_dev		**6**	**0.83**	**4.75**	**6.15**		**0.79**	**6.89**	**1.66**	**0.18**
	SNV		12	0.79	5.32	7.67		0.77	7.06	1.62	-0.69

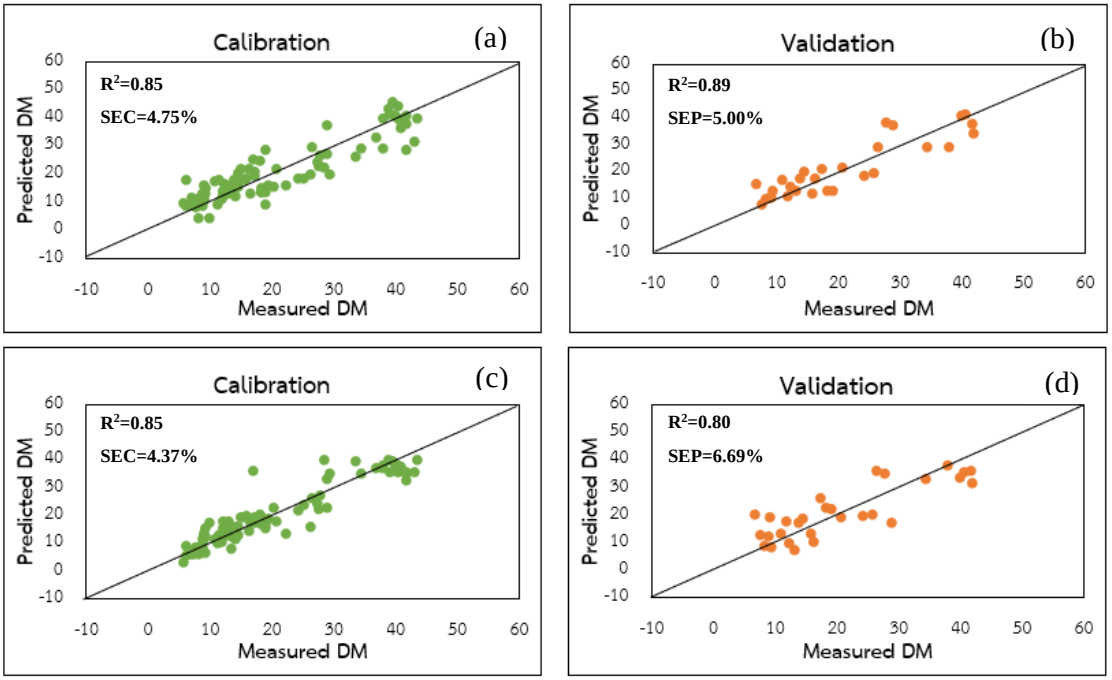

Figure 8 Scatter plots between measured and predicted value in the prediction of DM of durian a) LWNIR of the calibration set, b) LWNIR of the test set, c) SWNIR of the calibration set, and d) SWNIR of the test set.

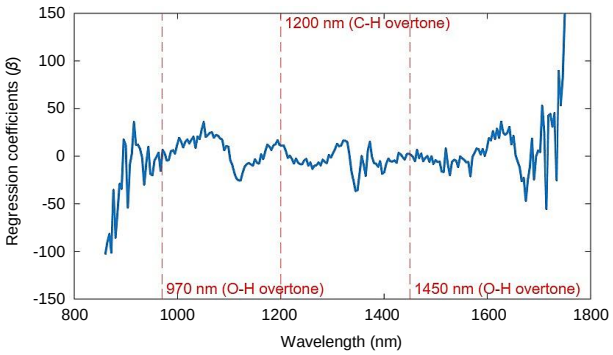

Figure 9 Regression coefficients of the PLSR model for predicting durian DM.

The experimental results and a comparison with previous studies show that for contact-based measurements, scanning durians with the spikes removed (to create a flat surface) yields better results than scanning without removing the spikes. However, if nondestructive scanning of the whole durian fruit is preferred, without cutting the spikes, then a non-contact measurement method should be used. Therefore, appropriate preprocessing is necessary. Specifically, applying the second derivative can reduce the baseline effects and enhance the clarity of important peaks. This approach reduces the influence of spikes and provides better model performance, as demonstrated by our experimental results. The resulting spectra represent the entire fruit, demonstrating that this method can be applied for online DM measurements of durians as they move along a conveyor belt.

4. Conclusions

The proposed method enables online assessment of durian fruit quality based on DM, categorizing them into two groups: rejected (DM < 32%) and accepted (DM ≥ 32%). The model performed well when developed using a balanced dataset for LWNIR and SWNIR spectra. The most effective approach for model development, based on conveyor belt scanning, was derived from LWNIR spectra using the 1st derivative-LDA, as it could be applied to both imbalanced and balanced datasets. The feasibility of classifying durian grades based on DM was confirmed by the PLSR model, which predicted DM with an r^2 of up to 0.80 for LWNIR and SWNIR. NIR spectroscopy demonstrated high potential for nondestructive classification of durian quality. Online quality grading on a conveyor belt can be implemented for quality control, particularly during the sorting process for produce in the durian export industry. It can also be applied to post-harvest quality assessment.

5. Acknowledgements

This work was also supported by Research and Graduate Studies, Khon Kaen University, Thailand. This research was supported by the Fundamental Fund of Khon Kaen University, Thailand, and has received funding support from the National Science, Research, and Innovation Fund, Thailand.

6. References

[1] Thai Government. Thai-Chinese trade is proceeding smoothly, with a target of exporting 700,000 tons of durian this year. [Internet]. 2023 [cited 2025 Feb 4]. Available from: https://archives.thaigov.go.th/th/t/34/media/infographic/view/7030.
[2] Matichon Online. Keep an eye on exporting 'Thai durian' to the Chinese market [Internet]. 2023 [cited 2025 Feb 4]. Available from: https://www.matichon.co.th/economy/news_3904043. (In Thai)
[3] Office of Agricultural Economics. Export statistics of fresh durian [Internet]. 2022 [cited 2025 Feb 4]. Available from: https://oae.go.th/home/article/386. (In Thai)
[4] Ministry of Agriculture and Cooperatives. Establishing agricultural product standards (TAS 9028-2557) [Internet]. 2014 [cited 2025 Feb 4]. Available from: https://www.ratchakitcha.soc.go.th/DATA/PDF/2557/E/200/7.PDF. (In Thai)
[5] National Bureau of Agricultural Commodity and Food Standards. Thai Agricultural Standard TAS 3-2013; Durian [Internet]. 2013 [cited 2025 Feb 4]. Available from: http://patricklepetit.jalbum.net/RAYONG/LIBRARY/durian-TIS.pdf.
[6] Posom J, Soonnamtiang N, Kotethum P, Konjun P, Sirisomboon P, Saengprachatanarug K, et al. Two different portables visible-near infrared and shortwave infrared region for on-tree measurement of soluble solid content of Marian plum fruit. Eng J. 2020;24(5):227-36.
[7] Maraphum K, Ounkaew A, Kasemsiri P, Hiziroglu S, Posom J. Wavelengths selection based on genetic algorithm (GA) and successive projections algorithms (SPA) combine with PLS regression for determination the soluble solids content in Nam-DokMai mangoes based on near infrared spectroscopy. Eng Appl Sci Res. 2022;49(1):119-26.
[8] Pourdarbani R, Sabzi S, Arribas JI. Nondestructive estimation of three apple fruit properties at various ripening levels with optimal Vis-NIR spectral wavelength regression data. Heliyon. 2021;7(9):e07942.
[9] Martins JA, Rodrigues D, Cavaco AM, Antunes MD, Guerra R. Estimation of soluble solids content and fruit temperature in 'Rocha' pear using Vis-NIR spectroscopy and the SpectraNet–32 deep learning architecture. Postharvest Biol Technol. 2023;199:112281.
[10] Malai C, Maraphum K, Saengprachatanarug K, Wongpichet S, Phuphaphud A, Posom J. Effective measurement of starch and dry matter content in fresh cassava tubers using interactance Vis/NIR spectra. J Food Compos Anal. 2024;125:105783.
[11] Posom J, Maraphum K. Achieving prediction of starch in cassava (*Manihot esculenta Crantz*) by data fusion of Vis-NIR and Mid-NIR spectroscopy via machine learning. J Food Compos Anal. 2023;122:105415.
[12] Maraphum K, Saengprachatanarug K, Wongpichet S, Phuphuphud A, Posom J. Achieving robustness across different ages and cultivars for an NIRS-PLSR model of fresh cassava root starch and dry matter content. Comput Electron Agric. 2022;196:106872.
[13] Tipsod N, Santalunai W, Posom J, Phuphaphudand A, Saengprachatanarug K. The low cost spectrometer for estimation of dry matter in fresh cassava tuber. Ag Bio Eng. 2024;1(4):108-12.

[14] Onsawai P, Phetpan K, Khurnpoon L, Sirisomboon P. Evaluation of physiological properties and texture traits of durian pulp using near-infrared spectra of the pulp and intact fruit. Measurement. 2021;174:108684.
[15] Sharma S, Sirisomboon P, Sumesh KC, Terdwongworakul A, Phetpan K, Kshetri TB, et al. Near-infrared hyperspectral imaging combined with machine learning for physicochemical-based quality evaluation of durian pulp. Postharvest Biol Technol. 2023;200:112334.
[16] Ali MM, Hashim N, Shahamshah MI. Durian (*Durio zibethinus*) ripeness detection using thermal imaging with multivariate analysis. Postharvest Biol Technol. 2021;176:111517.
[17] Saechua W, Sharma S, Nakawajana N, Leepaitoon K, Chunsri R, Posom J, et al. Integrating Vis-SWNIR spectrometer in a conveyor system for in-line measurement of dry matter content and soluble solids content of durian pulp. Postharvest Biol Technol. 2021;181:111640.
[18] Phuangsombut K, Phuangsombut A, Talabnark A, Terdwongworakul A. Empirical reduction of rind effect on rind and flesh absorbance for evaluation of durian maturity using near infrared spectroscopy. Postharvest Biol Technol. 2018;142:55-9.
[19] Ditcharoen S, Sirisomboon P, Saengprachatanarug K, Phuphaphud A, Rittiron R, Terdwongworakul A, et al. Improving the non-destructive maturity classification model for durian fruit using near-infrared spectroscopy. Artif Intell Agric. 2023;7:35-43.
[20] Phanomsophon T, Jaisue N, Worphet A, Tawinteung N, Shrestha B, Posom J, et al. Rapid measurement of classification levels of primary macronutrients in durian (*Durio zibethinus* Murray CV. Mon Thong) leaves using FT-NIR spectrometer and comparing the effect of imbalanced and balanced data for modelling. Measurement. 2022;203:111975.
[21] Zhang Z, Liu H, Chen D, Zhang J, Li H, Shen M, et al. SMOTE-based method for balanced spectral nondestructive detection of moldy apple core. Food Control. 2022;141:109100.
[22] Tongdee SC, Suwanagul A, Neamprem S. Durian fruit ripening and effect of variety, maturity stage at harvest, and atmospheric gases. Acta Hortic. 1990;269:323-34.
[23] Buasub W. Agricultural extension academic manual (Durian) [Internet]. 2007 [cited 2025 Feb 4]. Available from: https://agkb.lib.ku.ac.th/doae/search_detail/result/282214. (In Thai)
[24] Williams PC. Implementation of near-infrared technology. In: Williams PC, Norris KH, editors. Near-infrared technology in the agricultural and food industries. 2nd ed. Saint Paul: AACC Inc; 2001:145-71.
[25] Onsawai P, Sirisomboon P. Determination of dry matter and soluble solids of durian pulp using diffuse reflectance near-infrared spectroscopy. J Near Infrared Spectrosc. 2015;23(3):167-79.
[26] Matharaarachchi S, Domaratzki M, Muthukumarana S. Enhancing SMOTE for imbalanced data with abnormal minority instances. Mach Learn Appl. 2024;18:100597
[27] Liu D, Sun DW, Zeng XA. Recent advances in wavelength selection techniques for hyperspectral image processing in the food industry. Food Bioprocess Technol. 2014;7:307-23.
[28] Award M, Khanna R. Support vector regression. In: Award M, Khanna R, editors. Efficient Learning Machines. Berkeley: Apress; 2015. p. 67-80.
[29] Sutton O. Introduction to k nearest neighbour classification and condensed nearest neighbour data reduction [Internet]. 2012 [cited 2025 Feb 4]. Available from: https://www.semanticscholar.org/paper/Introduction-to-k-Nearest-Neighbour-Classification-Sutton/5aa3c91b59709bf9bbd4d9d856e1a10d79c9494f?utm_source=chatgpt.com.
[30] Brownlee J. Why use ensemble learning? [Internet]. 2021 [cited 2025 Feb 4]. Available from: https://machinelearningmastery.com/why-use-ensemble-learning.
[31] Wu H, Song Z, Niu X, Liu J, Jiang J, Li Y. Classification of *Toona sinensis* Young Leaves Using Machine Learning and UAV-Borne Hyperspectral Imagery. Front Plant Sci. 2022;13:940327.
[32] Shajihan N. Classification of stages of diabetic retinopathy using deep learning [Internet]. 2020 [cited 2025 Feb 4]. Available from: https://www.researchgate.net/publication/347447352_Classification_of_stages_of_Diabetic_Retinopathy_using_Deep_Learning.
[33] Zornoza R, Guerrero C, Mataix-Solera J, Scow KM, Arcenegui V, Mataix-Beneyto J. Near infrared spectroscopy for determination of various physical, chemical and biochemical properties in Mediterranean soils. Soil Biol Biochem. 2008;40(7):1923-30.
[34] Benelli A, Cevoli C, Fabbri A, Ragni L. Ripeness evaluation of kiwifruit by hyperspectral imaging. Biosyst Eng. 2021;223:42-52.
[35] Osborne BG, Fearn T, Hindle PH. Practical NIR spectroscopy with applications in food and beverage analysis. Harlow: Longman Scientific and Technical; 1993.
[36] Burns DA, Ciurczak EW. Handbook of near-infrared analysis. 3rd ed. Boca Raton: CRC Press; 2007.
[37] Somton W, Pathaveerat S, Terdwongworakul A. Application of near infrared spectroscopy for indirect evaluation of 'Monthong' durian maturity. Int J Food Prop. 2015;18(6):1155-68.
[38] Sharma S, Sumesh KC, Sirisomboon P. Rapid ripening stage classification and dry matter prediction of durian pulp using a pushbroom near infrared hyperspectral imaging system. Measurement. 2022;189:110464.
[39] Sirisomboon P, Funke A, Posom J. Improvement of proximate data and calorific value assessment of bamboo through near infrared wood chips acquisition. Renew Energy. 2020;147:1921-31.
[40] Cen H, He Y. Theory and application of near infrared reflectance spectroscopy in determination of food quality. Trends Food Sci Technol. 2007;18(2):72-83.
[41] Taskiran SF, Turkoglu B, Kaya E, Asuroglu T. A comprehensive evaluation of oversampling techniques for enhancing text classification performance. Sci Rep. 2025;15:21631.
[42] Talabnark A, Terdwongworakul A. Minimally destructive evaluation of durian maturity using near infrared spectroscopy. Thai Soc Agric Eng J. 2017;23(2):9-16. (In Thai)
[43] Timkhum P, Terdwongworakul A. Non-destructive classification of durian maturity of 'Monthong' cultivar by means of visible spectroscopy of the spine. J Food Eng. 2012;112(4):263-7.
[44] Puttipipatkajorn A, Terdwongworakul A, Puttipipatkajorn A, Kulmutwat S, Sangwanangkul P, Cheepsomsong T. Indirect prediction of dry matter in durian pulp with combined features using miniature NIR Spectrophotometer. IEEE Access. 2023;11:84810-21.